DOI: 10.1002/ejic.201000962

Dinuclear Tris(1-pyrazolyl)methane Complexes of Ruthenium(II)

Massimo Guelfi,[a] Fausto Puntoriero,[b] Scolastica Serroni,[b] and Gianfranco Denti*[a]

Keywords: Ruthenium / Mixed-valent compounds / Electrochemistry / Dinuclear complexes / Polypyridine complexes

By exploiting the "complexes-as-metals/complexes-as-ligands" synthetic strategy, six new dinuclear achiral complexes of Ru^{II}, containing the tripodal ligand tris(1-pyrazolyl)methane (tpm), a chelating ligand (L-L) such as 2,2′-bipyridine (2,2′-bpy), 1,10-phenanthroline (phen) or 2,2′-biquinoline (biq), and either pyrazine (pz) or 4,4′-bipyridine (4,4′-bpy) as bridging ligands (BL), have been prepared and fully characterized. The starting building blocks, many of which have been synthesized for the first time, have been conveniently prepared by improved literature methods. The reactivity of these building blocks in specific experimental conditions has been rationalized. All novel compounds have been characterized fully by elemental analysis and FT-IR. ^{1}H NMR spectra have been carefully assigned and interpreted on the basis of possible inductive and magnetic anisotropic effects exerted by the ligands. Electrochemical, UV/Vis spectroscopic, and luminescence studies have been carried out on all the dinuclear complexes and their precursor species; the collected data have been discussed and thoroughly interpreted. Ru^{II}/Ru^{III} mixed-valence species of two dinuclear compounds have been investigated by spectroelectrochemistry and assigned to the Robin and Day's Class II group on the basis of the experimental parameters obtained.

Introduction

After more than two decades of intensive study mono- and oligo-nuclear ruthenium(II) complexes in which all ligands are N-donor azaarenes, which are often called polypyridyl or polypyridine complexes, and contain RuN$_6$ entities, are still attracting the attention of several research groups, mainly because of their well defined electrochemical and photophysical properties that can be exploited in several different ways.[1]

Our previous work[2] on the synthesis of large polypyridine systems based on [Ru(2,3-dpp)$_3$]$^{2+}$ and [Os(2,3-dpp)$_3$]$^{2+}$ units (2,3-dpp = 2,3-dipyridylpyrazine) gave rise to reasonable synthetic results that allowed us to study the outstanding electrochemical and photophysical properties of compounds with nuclearities up to 22. Nevertheless, the study was unsatisfactory from a structural point of view since tris-chelated species are chiral and thus oligonuclear compounds based on them are formed as diastereoisomeric mixtures, which prevents both solid state and solution based structural studies. Since this limitation can be overcome with synthons containing symmetric tridentate ligands, we decided to focus our work in this direction.

Tridentate ligands have been employed to prepare RuN$_6$ species with either a meridional or a facial coordination geometry. The complexes of first type are mainly based on 2,2′:6′,2′′-terpyridine or 2,4-di(2-pyridyl)-1,3,5-triazine derivatives and are widely represented in the literature.[3] On the contrary examples of RuN$_6$ complexes containing tripodal ligands are quite scarce.

So far, only two polypyridyl complexes containing η^3-hydrotris(1-pyrazolyl)borate (Tp) have been reported in the literature,[4] and those containing tris(2-pyridyl)methane (tpym) are only represented by the bis-coordinated [Ru(tpym)$_2$](tosylate)$_2$.[5] Examples of Ru^{II} polypyridine complexes containing tris(1-pyrazolyl)methane (tpm) acting as a η^3 ligand are not as numerous as it might be expected.[6] Approximately a dozen of these compounds have been reported in the literature, including [Ru(tpm)(2,2′-bpy)(py)](PF$_6$)$_2$ (2,2′-bpy = 2,2′-bipyridine and some analogous ligands disubstituted at the 4 and 4′ positions; py = pyridine),[7] [Ru(tpm)(py)$_3$](PF$_6$)$_2$ (py = pyridine[8a] or 4-vinylpyridine[8b]), [Ru(tpm)(L-L)(py)](PF$_6$)$_2$ (L-L = dipyrido[3,2-*a*:2′,3′-*c*]phenazine and py = pyridine itself[9a] or three derivatives;[9b] L-L = benzo[*i*]dipyrido[3,2-*a*:2′,3′-*c*]phenazine, py = pyridine[9c]), [Ru(tpm)(2,2′-bpy)(BL)](PF$_6$)$_2$ (BL = pz, 4,4′-bpy, *trans*-1,2-di(4-pyridyl)ethylene;[10] 4-pyridinecarboxaldehyde azine;[11a] 4,4′-azobis(pyridine)[11b]). The dinuclear species[{Ru(tpm)(2,2′-bpy)}$_2$(μ-4,4′-dipyridyl-1,5-pentane)](PF$_6$)$_4$ containing a long bridging unit has also been synthesized.[12]

In view of what is already known, we decided to use synthons containing the Ru(tpm) subunit in order to build di- and oligo-nuclear achiral complexes. We exploited our "complexes-as-metals/complexes-as-ligands" synthetic ap-

---

[a] Inorganic Chemistry Laboratory, Faculty of Agriculture,
University of Pisa,
56124 Pisa, Italy
Fax: +39-050-2216630
E-mail: Gianfranco.Denti@unipi.it
[b] Department of Inorganic Chemistry, Analytical Chemistry, and Physical Chemistry, University of Messina,
98166 Messina, Italy

Supporting information for this article is available on the WWW under http://dx.doi.org/10.1002/ejic.201000962 proach[2a] that is based on metathesis reactions between synthons containing one or more labile ligands (the "complex metals") and synthons bearing free nitrogen donors on already coordinated ligands that will act as bridges (the "complex ligands"). Either bis-monodendate or bis-chelating molecules can be employed as bridging ligands, and depending on which is present further chelating or monodentate ancillary ligands will complete the coordination sphere of the metal.

In this paper we report on the preparation of *symmetric* dinuclear species $[\{Ru(tpm)(L\text{-}L)\}_2(\mu\text{-}BL)]^{4+}$ (L-L = 2,2′-bpy, phen, biq; BL = pz, 4,4′-bpy; see Scheme 1 and Figure 1), which are obtainable from the complex metals $[Ru(tpm)(L\text{-}L)(H_2O)]^{2+}$ and the complex ligands $[Ru(tpm)(L\text{-}L)(BL)]^{2+}$. In order to find the best preparative procedures different experimental conditions have been investigated in relation to different supposed reaction mechanisms. (*Asymmetric* dinuclear complexes have also been synthesized and are under electrochemical and photophysical investigation. They will be the subject of a subsequent paper. The synthesis of higher functionality complex ligands, such as $[Ru(tpm)(4,4'\text{-}bpy)_3]^{2+}$, suitable for preparing tetranuclear compounds, will be also performed.)

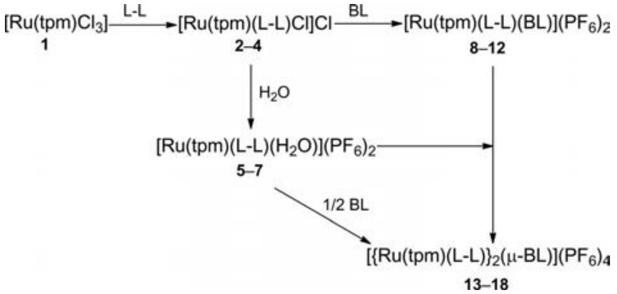

Scheme 1. Preparation scheme for the dinuclear complexes.

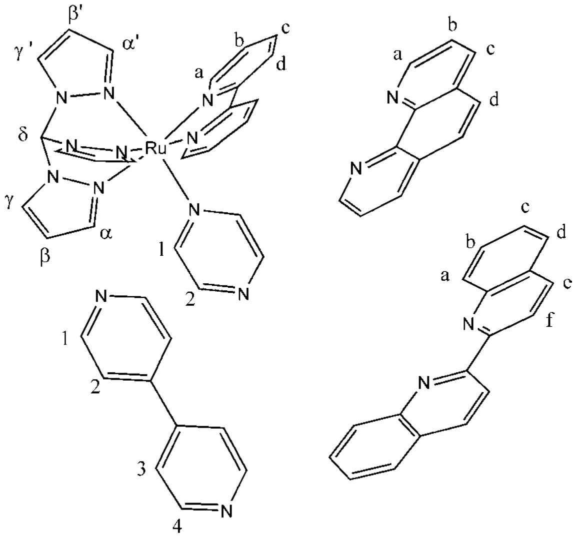

Figure 1. Ancillary and bridging ligands used in this work, showing atom labelling scheme for ^1H NMR assignments.

The spectroscopical, electrochemical, and luminescence properties of all reported species have been studied. Spectroelectrochemical experiments have been also performed on some dinuclear complexes in order to elucidate their mixed-valence properties.

Results and Discussion

Synthetic Studies

The complex metals [Ru(tpm)(L-L)Cl]Cl [L-L = 2,2′-bpy (**2**), phen (**3**), and biq (**4**)] were synthesized by a modified version of the procedure published by T. J. Meyer[13] who prepared **2** and **3** by refluxing an ethanol/water solution containing $Ru(tpm)Cl_3$ (**1**), the chelating ligand, and a large excess of LiCl; after few minutes, a large excess of triethylamine, a reducing agent, was added and the mixture refluxed for ten more minutes. In spite of the reported yields for this method (41 and 66%, respectively) we were not able to obtain satisfactory results since the final reaction mixtures were always heavily contaminated with by-products. It seemed to us that the presence of chloride ions in the reaction mixture was counterproductive, and the use of NEt_3 unnecessary. Thus we refluxed solutions containing only complex **1** and the appropriate chelating ligands and obtained much better results.

The complex ligands **8**–**11** (see Table 1) were synthesized in good yields from the corresponding complex metals **2** and **3** by reaction of these complexes with large excesses of pz or 4,4′-bpy in a refluxing ethanol/water (3:1) solution. The reaction mechanism most likely involves the initial metathesis of the chloride ion with a water molecule. It is noteworthy that under the same conditions the biq analogues $[Ru(tpm)(biq)(pz)](PF_6)_2$ and $[Ru(tpm)(biq)(4,4'\text{-}bpy)](PF_6)_2$ cannot be obtained, even if much longer reaction times are employed; indeed, the reactions stop at the aquo species stage. The strong electron withdrawing force exerted by biq may make the substitution of the coordinated water molecule very hard under the specific reaction conditions; furthermore, in case of a dissociative mechanism, the aqueous medium could make the equilibrium position very unfavorable. Complex Rubiq-bpy (**12**) was prepared by treating $[Ru(tpm)(biq)(H_2O)](PF_6)_2$ (**7**) with an excess of 4,4′-bpy in refluxing absolute ethanol. The yield was limited by the formation of the corresponding dinuclear compound. The same procedure did not work at all for the synthesis of $[Ru(tpm)(biq)(pz)](PF_6)_2$, probably on account of the smaller nucleophilic character of free pz with respect to 4,4′-bpy, which may be further decreased by hydrogen bonding with the solvent.

The dinuclear complexes **13**–**16** and **18** can be prepared either by reacting the complex metals **5**–**7** with the appropriate complex ligands in a 1:1 molar ratio, or by reacting them with the free bridging ligands in a 2:1 molar ratio. The use of very mild conditions (dichloromethane solution, room temperature) requires rather long reaction times, but makes the reaction very clean so that the products that spontaneously precipitate do not require purification. Com-

Table 1. Numbers and short names for the synthesized complexes.

Formula		Short name
$[Ru(tpm)(2,2'\text{-bpy})(pz)](PF_6)_2$	**8**	Rubpy-pz
$[Ru(tpm)(2,2'\text{-bpy})(4,4'\text{-bpy})](PF_6)_2$	**9**	Rubpy-bpy
$[Ru(tpm)(phen)(pz)](PF_6)_2$	**10**	Ruphen-pz
$[Ru(tpm)(phen)(4,4'\text{-bpy})](PF_6)_2$	**11**	Ruphen-bpy
$[Ru(tpm)(biq)(4,4'\text{-bpy})](PF_6)_2$	**12**	Rubiq-bpy
$[\{Ru(tpm)(2,2'\text{-bpy})\}_2(\mu\text{-pz})](PF_6)_4$	**13**	$(Rubpy)_2$-pz
$[\{Ru(tpm)(2,2'\text{-bpy})\}_2(\mu\text{-}4,4'\text{-bpy})](PF_6)_4$	**14**	$(Rubpy)_2$-bpy
$[\{Ru(tpm)(phen)\}_2(\mu\text{-pz})](PF_6)_4$	**15**	$(Ruphen)_2$-pz
$[\{Ru(tpm)(phen)\}_2(\mu\text{-}4,4'\text{-bpy})](PF_6)_4$	**16**	$(Ruphen)_2$-bpy
$[\{Ru(tpm)(biq)\}_2(\mu\text{-pz})](PF_6)_4$	**17**	$(Rubiq)_2$-pz
$[\{Ru(tpm)(biq)\}_2(\mu\text{-}4,4'\text{-bpy})](PF_6)_4$	**18**	$(Rubiq)_2$-bpy

plex $(Rubiq)_2$-pz (**17**) can be prepared only by the second procedure reported above owing to the unavailability of the corresponding complex ligand. Attempts to synthesize the latter complex in dichloromethane from the aquo species and a large excess of pz failed, and the dinuclear compound was always obtained. This result should confirm that, in this specific case, the initial reactivity of pz is strongly influenced by the possible formation of hydrogen bonds, and that the first coordination of pz hugely increases the basic strength of the second nitrogen atom.[14]

NMR Spectra

All products were characterized by ^1H NMR spectroscopy (see Exp. Sect.).

The spectra can be unambiguously assigned on the basis of the multiplicities of the signals, thanks to the molecular symmetries: the hydrogen atoms of two pyrazole rings of tpm, and those of the two symmetric moieties of the chelating ligands that are in *trans* positions to the aforementioned tpm rings, are always equivalent. Furthermore, the coupling constants of hydrogen atoms on five-membered rings are smaller than those for hydrogen atoms on six-membered rings, which helps the attribution of the tpm signals; the comparison of mononuclear and dinuclear systems allows for the detection of the signals arising from the BL protons.

Figure 2 shows the interpreted spectra of complexes Ruphen-pz (**10**) and $(Ruphen)_2$-pz (**15**) that are representative examples of mono- and dinuclear analogous species. The interpreted spectra of compounds **8**, **9**, **11**–**14**, and **16**–**18** are reported in the Supporting Information.

The coordination of tpm to a Ru(L-L)(BL) subunit influences the chemical shift of its hydrogen atoms, each to a different extent. In spite of its relatively long distance from the metallic centre, the methine hydrogen at the δ position (see Figure 1) experiences the largest effect, being deshielded by 1.08–1.91 ppm with respect to the free ligand (in $[D_6]$acetone solution the signal is observed at $\delta = 8.74$ ppm for the free ligand and at $\delta = 9.82$–10.65 ppm for the coordinated ligand). Apart from possible changes to the magnetic anisotropy subsequent to coordination, apparently the inductive effect on this benzyl-like position is particularly efficient because it is mediated by three aromatic rings, and parallels the combined influence of the ancillary and bridging ligands on the Ru ion; this effect is at a maximum in case of compound $(Rubiq)_2$-bpy (**18**). This particular result might be explained by taking into account that, while in mononuclear complexes pz proves to be a better π-acceptor (and a worse σ-donor) than 4,4′-bpy, the second coordination of the ligand strongly reduces the π-acidity of pz but does not affect much 4,4′-bpy.

It is noteworthy that the solvent also has a large effect on the chemical shift of H_δ: in general a shift of more than 0.70 ppm to lower frequencies is observed when the samples were dissolved in $[D_3]$acetonitrile instead of $[D_6]$acetone. Moreover the H_δ signal for complex $(Rubiq)_2$-pz (**17**) in $[D_6]$dimethyl sulfoxide, instead of $[D_6]$acetone, was shifted by 2.28 ppm to a higher frequency, which is a much larger chemical shift than observed for the other hydrogen atoms of tpm. These data, together with the H/D exchange that we observed for some complexes when in $[D_4]$methanol solution, confirm that the methine hydrogen is acidic in nature[15] and that its chemical shift moves to higher frequencies as the hydrogen bonding capability of the solvent increases.

The chemical shifts of the other hydrogen atoms of tpm mainly move to higher frequencies subsequent to coordination. The largest and not very variable changes are exhibited by H_γ and $H_{\gamma'}$ (shifted from 7.86 ppm for the free ligand in $[D_6]$acetone to 8.73–9.00 ppm and 8.56–8.91 ppm when complexed, respectively). Atom H_β is slightly deshielded (its signal is shifted from 6.41 ppm for the free ligand to 6.64–6.98 ppm when the ligand is bound); atom $H_{\beta'}$ is a little shielded (6.21–6.40 ppm) in Ruphen-pz (**10**), Ruphen-bpy (**11**), $(Rubpy)_2$-pz (**13**), $(Ruphen)_2$-pz (**15**), and $(Ruphen)_2$-bpy (**16**) and also a little deshielded (6.45–6.60 ppm) in Rubpy-pz (**8**), Rubpy-bpy (**9**), Rubiq-bpy (**12**), $(Rubpy)_2$-bpy (**14**), $(Rubiq)_2$-pz (**17**), and $(Rubiq)_2$-bpy (**18**). The H_α protons are significantly deshielded (their signal is shifted from 7.63 ppm for the free ligand to 8.17–8.60 ppm when the ligand is complexed, with the exception of Rubpy-pz when the signal is seen at 7.59 ppm), while the $H_{\alpha'}$ protons are generally shielded (6.33–7.29 ppm), but not when L-L = biq (in this case the chemical shifts remain practically unchanged). All these observations might be rationalized in terms of an interplay between magnetic anisotropy and inductive effects: the latter is due to the *trans* influences of the L-L and BL ligands and is expected to act as a deshielding factor towards the protons, and decreases in strength in the order $H_\alpha > H_\gamma > H_\beta$; the former, which is due to ring currents in the L-L ligands, sometimes result in large shielding of the $H_{\alpha'}$, the proton nearest to the average plane of the L-L ligand, which falls in its shielding cone, and could also have some shielding influence on $H_{\beta'}$. These data, together with those regarding the L-L and BL protons (see below) strongly support the hypothesis that tpm mainly behaves as σ-donor ligand. Similar reasons could be advanced in order to interpret the chemical shift changes observed for the hydrogen atoms of L-L ligands.

In general, some displacements (≤ 0.5 ppm) to higher frequencies are observed for all protons of 2,2′-bpy and

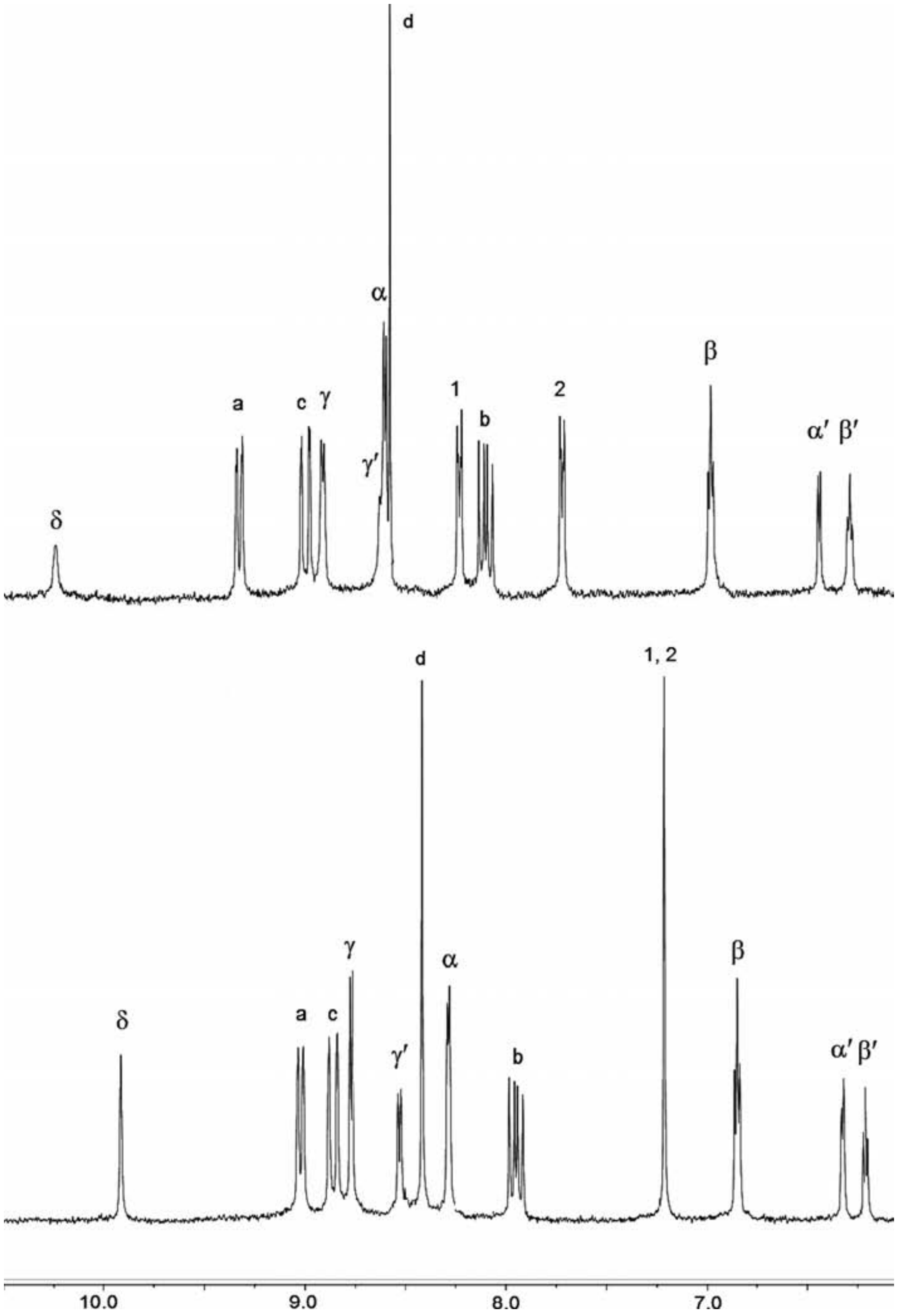

Figure 2. ^{1}H NMR spectra of $[Ru(tpm)(phen)(pz)]^{2+}$ (**10**, top) and $[\{Ru(tpm)(phen)\}_2(\mu\text{-}pz)]^{4+}$ (**15**, bottom) in [D$_6$]acetone. Labels refer to Figure 1.

phen. In the biq complexes Rubiq-bpy (**12**), (Rubiq)$_2$-pz (**17**), and (Rubiq)$_2$-bpy (**18**) the H$_a$ protons undergo large displacements to lower frequencies with respect to the signal for the uncoordinated ligand (a shift from 8.23 ppm to 6.74–6.82 ppm when the spectra are recorded in [D$_6$]acetone). This result does not seem explicable in terms of only an increase in the electron density of the rings due to the high π-accepting capability of biq. Indeed, each H$_a$ proton is near to the pyrazole at a *cis* position and falls in a strongly shielding zone the effect of which is enhanced because of the distorted coordination geometry of biq. (Due to steric hindrance, in octahedral and square planar transition metal complexes the coordination plane of biq is rotated some 20° away from the basal plane of the metal coordination polyhedron and adopts a sort of "butterfly" look with the individual quinolinic moieties subtending a dihedral angle of about 10° with respect to each other.[15d]) The same cause might explain the shielding of H$_e$ and H$_f$ by BL; the displacement of the signals for these protons to lower frequencies is smaller than the displacements seen for protons H$_a$ on account of the rotation of BL that averages the effect.

The chemical shifts of the BL protons are influenced both by the complex nuclearity and by the nature of the L-L ligands. For both pz and 4,4′-bpy the second coordination causes a displacement to lower frequencies of the chemical shifts of all the protons, due to an increased electron density on the aromatic rings. The first coordination causes the same trend for pz, while it gives rise to deshielding of the H_1 protons in 4,4′-bpy, in agreement with the more effective σ-donor ability and the weaker π-acidity of this ligand with respect to uncoordinated pz.

Electrochemistry

Electrochemical measurements (Table 2) indicate that the complexes under investigation undergo several redox processes in the potential range examined (+1.8/–1.8 V vs. SCE).

The oxidation processes are reversible for all species, with the exception of compound (Rubiq)$_2$-pz (**17**). All mononuclear complexes were oxidized once in the investigated potential window. The dinuclear complexes (Rubpy)$_2$-pz (**13**) and (Ruphen)$_2$-pz (**15**) show two successive one-electron oxidation processes, while for the dinuclear complexes (Rubpy)$_2$-bpy (**14**), (Ruphen)$_2$-bpy (**16**) and (Rubiq)$_2$-bpy (**18**) a single oxidation process involving two electrons is observed. The reduction behaviour of the dinuclear complexes [except for (Rubiq)$_2$-bpy (**18**), which undergoes absorption onto the electrode] is also very rich, with several, sometimes overlapping, reduction processes recorded.

Oxidation. The electrochemical properties of transition metal complexes are usually discussed with the assumption that both redox states involve electron transfer that can be suitably represented, in an approximate way, by localized molecular orbital configurations.[19]

For Ru^{II}-polypyridine complexes, oxidation processes are known to be metal centred,[19] thus the potential values mainly depend on the electronic density that the coordinated ligands leave on the metal. The oxidation potentials reported in Table 2 account for this effect.

The oxidation of the mononuclear species Rubpy-pz (**8**), Ruphen-pz (**10**), Ruphen-bpy (**11**), and Rubiq-bpy (**12**) can be discussed with reference to model compounds [Ru(bpy)$_3$]$^{2+}$, [Ru(phen)$_3$]$^{2+}$, and [Ru(biq)$_3$]$^{2+}$, respectively. The species **8** and **10** are oxidized at a potential very similar to that at which the oxidation of the model compounds [Ru(2,2′-bpy)$_3$]$^{2+}$ and [Ru(phen)$_3$]$^{2+}$ occurs (see Table 2), probably because the electronic effects of pz (which is a better electron-acceptor than bpy and phen) and of the tripodal ligand (a worse electron-acceptor than bpy and phen) cancel each other out. Such an explanation also accounts for the oxidation values of the other mononuclear species: in general the tripodal ligand reduces the effects caused by the presence of more electron-withdrawing ligands.

Figure 3 shows the anodic region of the cyclic voltammograms for (Ruphen)$_2$-pz (**15**) and (Ruphen)$_2$-bpy (**16**), which are representative of the different behaviors exhibited by the dinuclear species, depending on the bridging ligand present. The dinuclear species (Rubpy)$_2$-pz (**13**) and (Ruphen)$_2$-pz (**15**) exhibit two successive one-electron oxidation processes, which suggest a good electronic communication through the pz bridge.[20] The oxidation of the first metal centre moves the oxidation of the second towards more positive potentials; for the same reason (Rubiq)$_2$-pz (**17**) shows only one one-electron oxidation process in the investigated potential window. On the contrary, in the voltammograms for the dinuclear species (Rubpy)$_2$-bpy (**14**), (Ruphen)$_2$-bpy (**16**), and (Rubiq)$_2$-bpy (**18**) the observed two-electron pro-

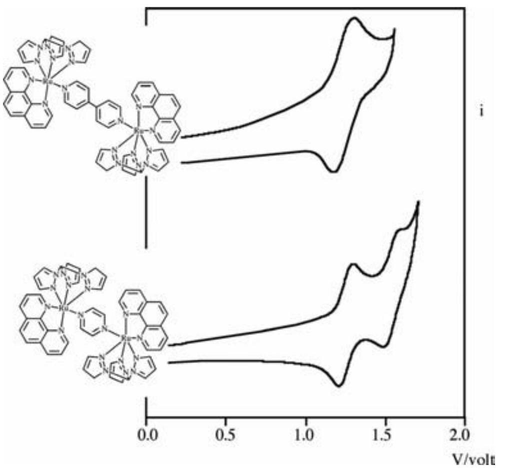

Figure 3. Anodic regions of the cyclic voltammograms of (Ruphen)$_2$-pz (**15**, bottom) and (Ruphen)$_2$-bpy (**16**, top), recorded at a scan rate of 200 mV s^{-1}.

Table 2. Electrochemical data[a] for mononuclear, dinuclear and reference complexes.

	Short name	$E_{1/2}^{ox}$	$E_{1/2}^{red}$		Short name	$E_{1/2}^{ox}$	$E_{1/2}^{red}$
8[b]	Rubpy-pz	+1.29 [1]	–1.41 [1]	**13**	(Rubpy)$_2$-pz	+1.29 [1]; +1.57 [1]	–1.17 [1]; –1.42 [1]; –1.52 [1]
9[b]	Rubpy-bpy	+1.21 [1]	–1.41 [1]	**14**	(Rubpy)$_2$-bpy	+1.23 [2]	–1.28 [1]; –1.42 [1]
10	Ruphen-pz	+1.31 [1]	–1.45 [1]	**15**	(Ruphen)$_2$-pz	+1.29 [1]; +1.57 [1]	–1.18 [1]; –1.44 [1]; –1.49[c]
11	Ruphen-bpy	+1.21 [1]	–1.37 [1]	**16**	(Ruphen)$_2$-bpy	+1.27 [2]	–1.30[d]; –1.43[d]
				17	(Rubiq)$_2$-pz	+1.38[d]	–0.92 [1]; –1.48 [1]; –1.76[d]
12	Rubiq-bpy	+1.31 [1]	–0.95 [1]; –1.53 [1]	**18**	(Rubiq)$_2$-bpy	+1.31 [2]	adsorption onto the electrode
Reference cations							
[Ru(2,2′-bpy)$_3$]$^{2+}$ [16]		+1.29 [1]	–1.33 [1]		[Ru(biq)$_3$]$^{2+}$ [18]	+1.47 [1]	–0.73 [1]
[Ru(phen)$_3$]$^{2+}$ [17]		+1.40 [1]	–1.41 [1]				

[a] Deareated acetonitrile solutions, r.t., 0.05 м tetraethylammonium hexafluorophosphate, V vs. SCE. Numbers printed in square brackets represent the number of electrons involved in each redox process. [b] From ref.[10] [c] Quasi-reversible process. [d] Irreversible process.

cesses are assigned to the simultaneous and independent one-electron oxidation of the two equivalent metal centres. This clearly indicates that the extent of the electronic coupling is poor, probably because the two pyridine subunits of the 4,4′-bpy ligand are not coplanar.

Reduction. The reduction processes are localized on the ligands, and their potential values reflect the energies of their π^* orbitals.

The mononuclear complexes Rubpy-pz (**8**) and Rubpy-bpy (**9**) are reduced at the same potential (–1.41 V vs. SCE). This suggests that the single reduction processes occurring in these complexes are localized on 2,2′-bpy. Their potentials are shifted to more negative values with respect to that of bpy in $[Ru(2,2'\text{-}bpy)_3]^{2+}$ (see Table 2), showing that the tripodal ligand acts as a good σ-donor and makes the metal center more electron-rich, considerably increasing the back-bonding towards the chelating ligand. However, on the basis of our experimental results, we cannot definitely exclude the possible involvement of the pz ligand in the reduction process of **8**. The same arguments account for the phen-centred reduction of Ruphen-pz (**10**) and Ruphen-bpy (**11**).

Two successive one-electron processes are observed in the voltammogram for Rubiq-bpy (**12**), the first is locatized on biq, which is suggested by comparison of the the potential value with the value recorded for the model compound $[Ru(biq)_3]$. The second reduction ought to be centred on 4,4′-bpy. This is not observed in the voltammogram for Ruphen-bpy, probably because it is shifted out of the potential window investigated by the reduction of phen at a more negative potential.

In the dinuclear species $(Rubpy)_2$-pz (**13**) the π^* orbitals of pz are stabilized by the second metal coordination, so the first reduction can be localized on the bridge, while the second and third reduction processes involve the two peripheral 2,2′-bpy ligands. Actually, the rather small difference between the first and the second reduction potentials (250 mV, see Table 2) would exclude the possibility that the second process could still involve the pz bridge, as electron pairing in pyrazine ligands is expected to require a potential decrease of much more than 400 mV.[19] Interestingly, the second and third reduction processes occur at different potentials, although the two 2,2′-bpy ligands are chelated to different metal centres, which accounts for a significant electronic coupling between them, as also indicated by the splitting of the oxidation potentials (see above). Furthermore, it can be noted that a doubly reduced state with an added electron on each 2,2′-bpy ligand should be more stable, for columbic reasons, than a doubly reduced state with one electron added to the pz bridge and one electron added to a 2,2′-bpy ligand. On this basis, it might be proposed that after the first electron is added to the pz bridge, the addition of the second one to a bpy ligand causes an electron shifting from pz to the other bpy ligand (formally a pz-to-bpy electron transfer). Then the third reduction should again involve the pz bridging ligand; the potential difference (350 mV) between the first and the third reduction (both involving a “neutral” pz subunit) would be related to columbic effects caused by the two reduced 2,2′-bpy ligands. Moreover, if this is the case, the difference between the second and the third reduction potentials could be explained without invoking any electronic coupling between the peripheral 2,2′-bpy sites. An analogous discussion could be considered for the reduction features observed in the voltammograms for $(Ruphen)_2$-pz (**15**) and $(Rubiq)_2$-pz (**17**), but taking into account that in the latter species the first reduction process involves a biq ligand.

The reduction of the 4,4′-bpy-bridged dinuclear species $(Rubpy)_2$-bpy (**14**) and $(Ruphen)_2$-bpy (**16**) can be rationalized by similar arguments. The addition of an electron to the bridge significantly changes its features and modifies the electronic communication that, as the oxidation data indicate, in the tetracation is negligible. For both species the expected third process is apparently shifted outside of our potential window. All of the above signal assignments are in agreement with the electrochemical data reported for other complexes containing 4,4′-bpy or pz as bridges.[20,21]

Table 3. Absorpion and photophysical data.

	Absorption[a] λ_{max} [nm] (ε [$M^{-1}cm^{-1}$])	Luminescence[b] λ_{max} [nm]	τ [µs]		Absorption[a] λ_{max} [nm] (ε [$M^{-1}cm^{-1}$])	Luminescence[b] λ_{max} [nm]	τ [µs]
8[c]	289 (54800)	570	6.5	**13**	296 (62000)	614	5.7
Rubpy-pz	390 (14400)			$(Rubpy)_2$-pz	406 (15000)		
					504 (27200)		
9[c]	395 (11000)	573	9.0	**14**	286 (65100)	596	5.8
Rubpy-bpy	286 (22000)			$(Rubpy)_2$-bpy	433 (22200)		
10	289 (45000)	580	6.0	**15**	290 (64000)	617	9.0
Ruphen-pz	372 (17000)			$(Ruphen)_2$-pz	368 (14000)		
					434 (23000)		
11	267 (57000)	575	9.5	**16**	266 (77100)	597	8.9
Ruphen-bpy	388 (16400)			$(Ruphen)_2$-bpy	390 (13800)		
					510 (23400)		
				17	265 (64800)	746	2.1
				$(Rubiq)_2$-pz	332 (46500)		
					556 (14800)		
12	265 (37900)	747	2.2	**18**	265 (74800)	745	2.0
Rubiq-bpy	333 (24500)			$(Rubiq)_2$-bpy	332 (48500)		
	555 (6350)				554 (15800)		

[a] In acetonitrile solutions at r.t. [b] In butyronitrile rigid matrix at 77 K. [c] From ref.[10]

UV/Vis Absorption Spectra

Absorption spectra (Table 3) exhibit very intense bands in the UV region and intense bands in the visible region. Figures 4 and 5 show the spectra of two representative couples of mononuclear / dinuclear species.

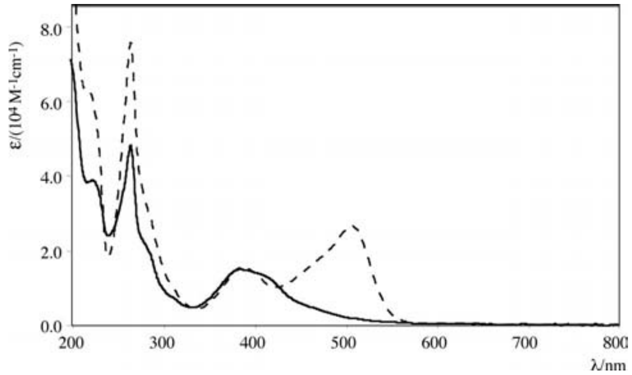

Figure 4. Absorption spectra for Ruphen-bpy (**11**, full line) and $(Ruphen)_2$-bpy (**16**, dashed line).

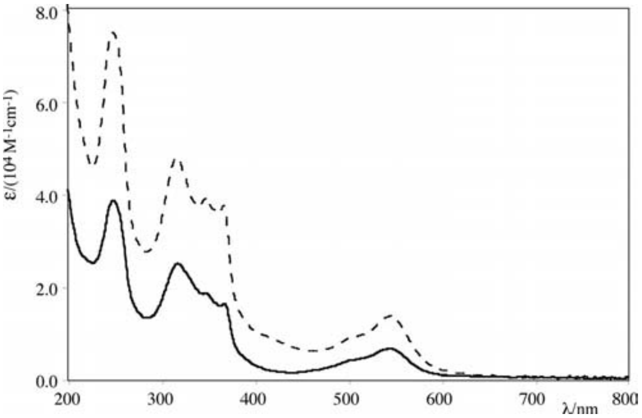

Figure 5. Absorption spectra for Rubiq-bpy (**12**, full line) and $(Rubiq)_2$-bpy (**18**, dashed line).

Previous investigations of related compounds[22] allow us to attribute the strong bands peaking at around 250 and 280 nm in the spectra to spin allowed polypyridine-centred (LC) transitions, and the broad absorptions between 310 and 600 nm mainly to many spin allowed Ru → polypyridine charge-transfer (MLCT) transitions.

Comparison of the absorption spectra of Ruphen-bpy (**11**) and $(Ruphen)_2$-bpy (**16**) (Figure 4) indicates that the second coordination of 4,4′-bpy stabilizes its π* orbital (as also shown by the electrochemical properties) allowing the population of a state of lowered energy, e.g. $Ru^{II} \rightarrow \mu$-4,4′-bpy (λ_{max} = 510 nm, ε = 23400 $M^{-1}\,cm^{-1}$). Analogous effects are observed for the couples Rubpy-pz (**8**) / $(Rubpy)_2$-pz (**13**) and Ruphen-pz (**10**) / $(Ruphen)_2$-pz (**15**) (see Table 3). On the contrary, the absorption profiles for Rubiq-bpy (**12**) and $(Rubiq)_2$-bpy (**18**) [and even that of $(Rubiq)_2$-pz (**17**)] are very much alike, as shown in Figure 5, because in these cases, in the mononuclear and dinuclear complexes the low lying MLCT states involve the peripheral biq ligands (see electrochemistry section).

Emission Spectra

All the investigated species do not exhibit any luminescence at 298 K in fluid acetonitrile solution. This behaviour is probably due to the lowering of the energy of the MC state with respect to that which is typical of analogues polypyridine complexes, as a consequence of an increased distortion in the octahedral geometry due to the presence of the tripodal ligand. Thus the MC state becomes closer in energy to the MLCT state, so that the thermally activated surface crossing to the MC state is made very efficient and finally leads to very fast radiationless decay.

Thermal population of the upper-lying MC states is not effective at 77 K, thus allowing for luminescence from the MLCT state, and all the species exhibit luminescence at 77 K in rigid matrix forms (see Table 3).

For the mononuclear complexes **8**–**12** the luminescence is attributed to the deactivation of ^{3}MLCT states involving the Ru^{II} center and the chelating ligand. In the case of the four dinuclear species **13**–**16**, which do not contain biq, the emission energy becomes lower with respect to the analogous mononuclear compounds (Table 3). This can be attributed to the second coordination of the bridging ligands that makes them easier to reduce with respect to the peripheral ligands. Figure 6 shows a comparison between a mononuclear and two dinuclear complexes of this group.

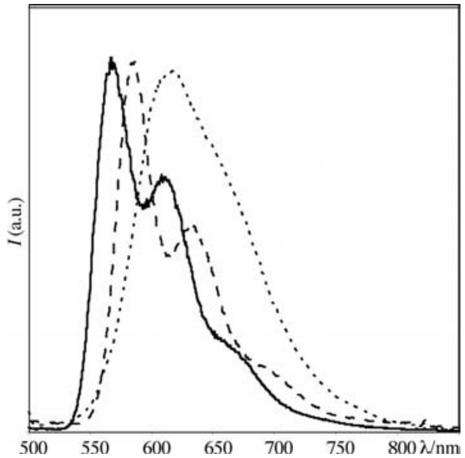

Figure 6. Emission spectra, recorded at 77 K in rigid matrices, for Ruphen-bpy (**11**, full line), $(Ruphen)_2$-pz (**15**, dotted line), and $(Ruphen)_2$-bpy (**16**, dashed line).

It is worthy of note that the emission spectra of the dinuclear compounds $(Rubpy)_2$-pz (**13**) and $(Ruphen)_2$-pz (**15**) are structureless, while all the other investigated species show structured luminescence profiles. Highly structured MLCT emission spectra are associated with negligible displacements of the excited-state nuclear coordinates compared to the ground state coordinates.[23,24] This suggests that the emitting MLCT states for these complexes have very different geometries compared to their ground states. Probably in these species the shorter metal-metal distances with respect to that of the μ-4,4′-bpy analogues, due to the presence of the pz bridging ligand, enhances the steric hindrance around the metal centers.

The emission features in the spectra for the complexes that contain biq, namely (Rubiq)$_2$-pz (**17**) and (Rubiq)$_2$-bpy (**18**) (Figure 7), are very similar to features seen in the spectrum of the mononuclear analogue Rubiq-bpy (**12**), suggesting that in both cases Ru^{II} → biq states are involved in the luminescence processes. This is in agreement with the electrochemical results that show that the biq ligand is easy to reduce with respect to the bridging ligand. Such a theory is further supported by the excited state lifetimes measured for Rubiq-bpy (**12**), (Rubiq)$_2$-pz (**17**), and (Rubiq)$_2$-bpy (**18**), which are typical of Ru^{II} → biq excited states[25] (μs timescale) and shorter than the values obtained for all the other species.

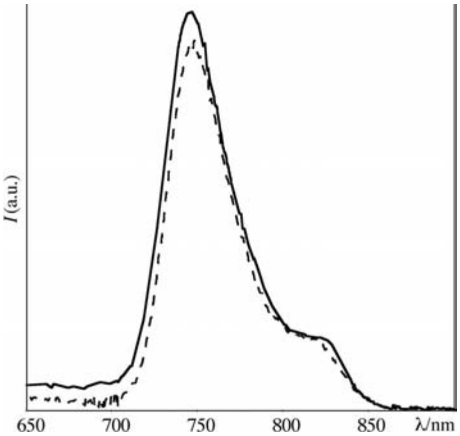

Figure 7. Emission spectra, recorded at 77 K in rigid matrices, for Rubiq-bpy (**12**, full line) and (Rubiq)$_2$-bpy (**18**, dashed line).

Spectroelectrochemistry

As shown in the electrochemistry section, the oxidation bands for the two metal centers in (Rubpy)$_2$-pz (**13**) and (Ruphen)$_2$-pz (**15**) are split. Such splitting, which indicates the relatively high stability of the mixed-valence species vs. the isovalent forms,[26] prompted us to investigate in more detail the properties of the corresponding mixed-valence forms, and to fulfil this aim spectroelectrochemical experiments were performed.

Figure 8 shows the change in the absorption spectrum of (Rubpy)$_2$-pz (**13**) on applying a potential of 1.30 V vs. SCE for a time sufficient to achieve the complete oxidation of the first metal center. A slight increase in absorption is observed in the infrared range (around 2100 nm), while a corresponding decrease in the intensity of the MLCT band at about 500 nm occurs. The new band appearing in the infrared region upon oxidation can be attributed to the Ru^{II} → Ru^{III} intervalence transfer (IT) transition. The symmetric shape of this band together with its width at half-height (3320 cm^{-1}) suggest that this species exhibits behavior typical of a Robin and Day's Class II type compound.[27]

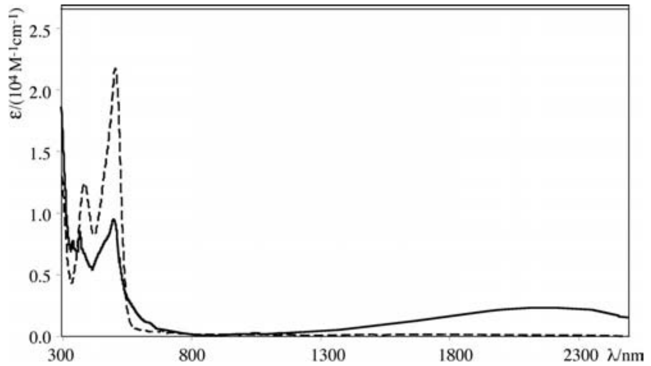

Figure 8. Absorption spectra for (Rubpy)$_2$-pz (**13**, dashed line) and mono-oxidized **13** (full line).

The same behaviour is exhibited by (Ruphen)$_2$-pz (**15**), as shown in Figure 9.

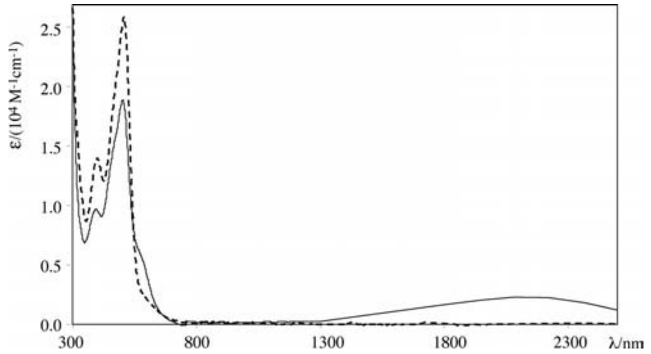

Figure 9. Absorption spectra for (Ruphen)$_2$-pz (**15**, dashed line) and mono-oxidized **15** (full line).

The formation of the IT bands in **13** and **15** allowed us to calculate the electronic interaction between the metal centres using the Hush Equation (1).[28]

$$\varepsilon_{max} = (2380\, d^2/\nu_{max}\, \Delta\nu_{1/2})\, H_{AB}^2 \qquad (1)$$

This equation correlates the optical intervalence transfer band to the magnitude of the electronic coupling matrix element between the two subunits A and B (in the present case, these are the Ru^{II} subunits), H_{AB}. In Equation (1), ε_{max} is the maximum molar absorption coefficient of the IT band, ν_{max} and $\Delta\nu$ are the band maximum energy and halfwidth (in cm^{-1}), and d is the intercomponent distance in Å. The values of above quantities are: for (Rubpy)$_2$-pz (**13**), ε_{max} = 1500 M^{-1}cm^{-1}, ν_{max} = 4665 cm^{-1}, $\Delta\nu$ = 3320 cm^{-1}, d = 6.6 Å (taken as the center-to-center distance obtained from simple energy minimization software[29]); for (Ruphen)$_2$-pz (**15**), ε_{max} = 1600 M^{-1}cm^{-1}, ν_{max} = 4650 cm^{-1}, $\Delta\nu$ = 3400 cm^{-1}, d = 6.6 Å. Application of these experimental parameters lead to a calculated value of about 470 cm^{-1} for H_{AB} in both cases. This value compares well with the electronic coupling matrix elements of dinuclear Ru^{II} polypyridine complexes bridged by good electron coupling mediator spacers such as cyanide[30] and pz[31] ligands (620 cm^{-1}), confirming the intense intercomponent interaction via the pz bridge in these complexes.

Conclusions

A series of mononuclear tris(1-pyrazolyl)methane-ruthenium(II) complexes containing a chelating ligand (2,2′-bpy, phen, biq) and a bridging ligand (pz, 4,4′-bpy) have been synthesized and used for the preparation of six symmetrical achiral dinuclear compounds by exploiting the "complexes-as-metals/complexes-as-ligands" synthetic strategy. ^{1}H NMR spectroscopy, electrochemical, UV/Vis and luminescence studies have allowed the role played by each component within the assembly to be recognized, confirming, in particular, that tpm essentially acts as a σ-donor ligand. Spectroelectrochemical experiments, when possible, have confirmed that in mixed-valence (II/III) species pz is a good electron coupling mediator between the metal centers. On the contrary, 4,4′-bpy does not help the intermetallic communication, which is probably reinforced in the +4 species by a lack of coplanarity of the two rings.

Future work will be aimed at the synthesis and study of the properties of asymmetric achiral dinuclear species, some of which have already been prepared. Increasing the nuclearity of the complexes will also be pursued.

Experimental Section

Materials, Methods and Instruments for Characterization: Solvents and other commercially available chemicals were used as received. Tpm[32] and [Ru(tpm)Cl$_3$] (**1**)[13] were prepared according to literature methods; the purification of tpm was accomplished by sublimation of the raw material at 11 Torr: at 25 °C the residual free pyrazole was removed, by heating to 90 °C very pure tpm was obtained. The complexes **2**–**4** were prepared from **1** by a heavily modified literature method[13] (see Results and Discussion). The corresponding aquo complexes **5**–**7** were prepared as hexafluorophosphate salts by a modification of the method reported in ref.[13] All reactions were carried out in an argon atmosphere with Schlenk techniques. Filtrations and purifications were usually performed in air. NMR spectra were obtained at 25 °C with a Varian Gemini NMR spectrometer operating at 200 MHz for ^{1}H with tetramethylsilane as internal reference. Infrared spectra (KBr pellets) were obtained with a Perkin–Elmer Spectrum RX I FT-IR spectrophotometer. Details of the preparation and characterization of complexes **2**–**7**, and NMR spectra of the complex ligands and dinuclear species are available as Electronic Supporting Information.

Syntheses of the Complex Ligands: The following procedures for the preparation of compounds **8** and **9**, when compared to a method already reported,[10] give considerably increased yields.

[Ru(tpm)(2,2′-bpy)(pz)](PF$_6$)$_2$ (8, Rubpy-pz): Compound **2** (0.100 g, 0.184 mmol) and pz (0.295 g, 3.68 mmol) were refluxed for 12 h in EtOH/H$_2$O, 3:1 (v/v, 25 mL). After cooling to room temperature the solution was concentrated, and a saturated aqueous solution of KPF$_6$ (ca. 3 mL) was added. The red solid obtained was filtered off, washed several times with cold water, and vacuum dried (yield 0.113 g, 73 %). $C_{24}H_{22}F_{12}N_{10}P_2Ru$ (842.04): calcd. C 34.26, H 2.64, N 16.64; found C 33.98, H 2.80, N 16.30. IR: ν_{max} = 1508 (m), 1458 (w), 1436 (w), 1406 (s), 1284 (m), 1249 (m), 1090 (m), 1056 (w), 780 (m), 751 (m), 606 (w), 520 (w) and 486 (w) cm^{-1}. ^{1}H NMR (200 MHz, [D$_6$]acetone, 20 °C): δ = 10.02 (s, 1 H, δ), 8.82 (d, $^{3}J_{H,H}$ = 8.8 Hz, 2 H, d), 8.75 (d, $^{3}J_{H,H}$ = 2.8 Hz, 1 H, γ′), 8.74 (d, $^{3}J_{H,H}$ = 2.8 Hz, 2 H, γ), 8.66 (d, $^{3}J_{H,H}$ = 8.8 Hz, 2 H, a), 8.18 (dd, $^{3}J_{H,H}$ = 8.1, 1.4 Hz, 2 H, 1), 7.66 (ddd, $^{3}J_{H,H}$ = 8.1, 7.0, 1.1 Hz, 2 H, b), 7.59 (d, $^{3}J_{H,H}$ = 2.2 Hz, 2 H, α), 7.29 (ddd, $^{3}J_{H,H}$ = 8.4, 7.0, 1.6 Hz, 2 H, c), 7.28 (d, $^{3}J_{H,H}$ = 2.2 Hz, 1 H, α′), 6.77 (dd, $^{3}J_{H,H}$ = 8.1, 1.6 Hz, 2 H, 2), 6.64 (dd, $^{3}J_{H,H}$ = 2.8, 2.3 Hz, 2 H, β), 6.48 (dd, $^{3}J_{H,H}$ = 2.9, 2.3 Hz, 1 H, β′) ppm.

[Ru(tpm)(2,2′-bpy)(4,4′-bpy)](PF$_6$)$_2$ (9, Rubpy-bpy): Compound **2** (0.100 g, 0.184 mmol) and 4,4′-bpy (0.575 g, 3.68 mmol) were refluxed for 12 h in EtOH/H$_2$O, 3:1 (v/v, 25 mL). After cooling to room temperature the solvent was removed by rotary evaporation. The solid thus obtained was washed several times with diethyl ether and dissolved in a minimum amount of water. Upon addition of a saturated aqueous solution of KPF$_6$ (ca. 3 mL) a red solid precipitated; this was filtered off, washed several times with diethyl ether, and vacuum dried (yield 0.129 g, 76 %). $C_{30}H_{26}F_{12}N_{10}P_2Ru$ (918.07): calcd. C 39.27, H 2.86, N 15.26; found C 39.33, H 2.69, N 15.03. IR: ν_{max} = 1597 (m), 1466 (m), 1447 (s), 1412 (s), 1287 (s), 1253 (m), 1229 (w), 1097 (s), 1059 (w), 994 (w), 761 (s), 731 (m), 629 (w), 608 (w) cm^{-1}. ^{1}H NMR (200 MHz, [D$_6$]acetone, 20 °C): δ = 9.89 (s, 1 H, δ), 9.10 (d, $^{3}J_{H,H}$ = 6.8 Hz, 2 H, 1), 9.05 (d, $^{3}J_{H,H}$ = 7.7 Hz, 2 H, d), 8.96 (d, $^{3}J_{H,H}$ = 5.4 Hz, 2 H, a), 8.82 (d, $^{3}J_{H,H}$ = 2.9 Hz, 2 H, γ), 8.61 (d, $^{3}J_{H,H}$ = 2.3 Hz, 1 H, γ′), 8.42–8.36 (overlapping multiplets, 4 H, α, c), 8.04 (dd, $^{3}J_{H,H}$ = 5.5, 1.4 Hz, 2 H, 4), 7.82 (dd, $^{3}J_{H,H}$ = 5.5, 1.5 Hz, 2 H, 3), 7.71 (overlapping multiplets, 4 H, 2, b), 6.99 (d, $^{3}J_{H,H}$ = 2.3 Hz, 1 H, α′), 6.93 (dd, $^{3}J_{H,H}$ = 2.8, 2.4 Hz, 2 H, β) 6.45 (dd, $^{3}J_{H,H}$ = 2.9, 2.3 Hz, 1 H, β′) ppm.

[Ru(tpm)(phen)(pz)](PF$_6$)$_2$ (10, Ruphen-pz): Compound **10** was obtained from **3**·CH$_2$Cl$_2$·H$_2$O (0.100 g, 0.149 mmol) and pz (0.240 g, 3.00 mmol) by the same procedure described for complex **8**. The product was obtained as a red solid (yield 0.101 g, 78 %). $C_{26}H_{22}F_{12}N_{10}P_2Ru$ (865.53): calcd. C 36.08, H 2.56, N 16.18; found C 35.98, H 2.80, N 15.90. IR: ν_{max} = 1603 (m), 1525 (w), 1467 (w), 1441 (m), 1420 (s), 1297 (s), 1255 (m), 1219 (w), 1160 (w), 1095 (s), 1067 (m), 1023 (w), 762 (s), 740 (m), 634 (w), 606 (w) cm^{-1}. ^{1}H NMR (200 MHz, [D$_6$]acetone, 20 °C): δ = 10.24 (s, 1 H, δ), 9.32 (dd, $^{3}J_{H,H}$ = 5.3, 1.3 Hz, 2 H, a), 8.99 (dd, $^{3}J_{H,H}$ = 8.2, 1.2 Hz, 2 H, c), 8.91 (d, $^{3}J_{H,H}$ = 2.8 Hz, 2 H, γ), 8.61 (d, $^{3}J_{H,H}$ = 2.8 Hz, 1 H, γ′), 8.60 (d, $^{3}J_{H,H}$ = 2.5 Hz, 2 H, α), 8.58 (s, 2 H, d), 8.23 (dd, $^{3}J_{H,H}$ = 3.2, 1.3 Hz, 2 H, 1), 8.10 (dd, $^{3}J_{H,H}$ = 8.2, 5.3 Hz, 2 H, b), 7.72 (dd, $^{3}J_{H,H}$ = 3.2, 1.3 Hz, 2 H, 2), 6.98 (dd, $^{3}J_{H,H}$ = 2.8, 2.5 Hz, 2 H, β), 6.44 (d, $^{3}J_{H,H}$ = 2.3 Hz, 1 H, α′), 6.28 (dd, $^{3}J_{H,H}$ = 2.8, 2.4 Hz, 1 H, β′) ppm.

[Ru(tpm)(phen)(4,4′-bpy)](PF$_6$)$_2$ (11, Ruphen-bpy): Compound **11** was obtained from **3**·CH$_2$Cl$_2$·H$_2$O (0.100 g, 0.149 mmol) and 4,4′-bpy (0.469 g, 3.00 mmol) by the same procedure described for complex **9**. The product was obtained as a red solid (yield 0.115 g, 81 %). $C_{32}H_{26}F_{12}N_{10}P_2Ru$ (942.07): calcd. C 40.82, H 2.78, N 14.88; found C 40.68, H 2.55, N 14.43. IR: ν_{max} = 1596 (m), 1427 (w), 1410 (m), 1286 (m), 1254 (m), 1096 (w), 1057 (m), 783 (w), 722 (w), 668 (w), 608 (w) cm^{-1}. ^{1}H NMR (200 MHz, [D$_6$]acetone, 20 °C): δ = 9.91 (s, 1 H, δ), 9.37 (dd, $^{3}J_{H,H}$ = 5.2, 1.0 Hz, 2 H, a), 8.98 (dd, $^{3}J_{H,H}$ = 8.2, 1.1 Hz, 2 H, c), 8.86 (d, $^{3}J_{H,H}$ = 2.8 Hz, 2 H, γ), 8.83 (dd, $^{3}J_{H,H}$ = 4.9, 1.4 Hz, 2 H, 1), 8.67 (d, $^{3}J_{H,H}$ = 2.3 Hz, 1 H, γ′), 8.58 (s, 2 H, d), 8.57 (d, $^{3}J_{H,H}$ = 2.7 Hz, 2 H, α), 8.09 (dd, $^{3}J_{H,H}$ = 8.2, 5.3 Hz, 2 H, b), 7.70 (dd, $^{3}J_{H,H}$ = 5.2, 1.5 Hz, 2 H, 4), 7.65 (dd, $^{3}J_{H,H}$ = 4.9, 1.5 Hz, 2 H, 2), 7.55 (dd, $^{3}J_{H,H}$ = 5.2, 1.4 Hz, 2 H, 3), 6.99 (dd, $^{3}J_{H,H}$ = 2.7, 2.4 Hz, 2 H, β), 6.42 (d, $^{3}J_{H,H}$ = 2.2 Hz, 1 H, α′), 6.28 (dd, $^{3}J_{H,H}$ = 2.9, 2.3 Hz, 1 H, β′) ppm.

[Ru(tpm)(biq)(4,4′-bpy)](PF$_6$)$_2$ (12, Rubiq-bpy): Compound **7** (0.050 g, 0.057 mmol) and 4,4′-bpy (0.176 g, 1.13 mmol) were refluxed for 12 h in absolute ethanol (25 mL). After cooling to room temperature the solution was concentrated, and an equal volume of diethyl ether was added. The mixture was stored overnight at –18 °C. A violet solid obtained and was filtered off, dissolved in a minimum amount of MeOH, and separated by column chromatography on silica (the eluant was MeOH saturated with KPF_6). The first violet fraction was discarded, but the second fraction (deep violet) was collected and dried by rotary evaporation. The solid obtained was suspended in water and extracted three times with CH_2Cl_2. The organic layer was dried with Na_2SO_4 and concentrated. On addition of diethyl ether a violet solid was obtained; this was separated by filtration, washed several times with diethyl ether, and vacuum dried (yield 0.033 g, 55%). $C_{38}H_{30}F_{12}N_{10}P_2Ru$ (1018.10): calcd. C 44.85, H 2.97, N 13.76; found C 44.98, H 2.69, N 13.61. IR: ν_{max} = 1596 (m), 1560 (m), 1508 (m), 1411 (m), 1286 (m), 1248 (w), 1110 (m), 1056 (w), 781 (m), 606 (w), 518 (w) cm^{-1}. ^{1}H NMR (200 MHz, [D$_6$]acetone, 20 °C): δ = 10.38 (s, 1 H, δ), 9.00 (d, $^3J_{H,H}$ = 2.4 Hz, 2 H, γ), 8.91 (d, $^3J_{H,H}$ = 2.3 Hz, 1 H, γ′), 8.86 (d, $^3J_{H,H}$ = 8.5 Hz, 2 H, 1), 8.76 (d, $^3J_{H,H}$ = 8.7 Hz, 2 H, 2), 8.69 (d, $^3J_{H,H}$ = 5.4 Hz, 2 H, 4), 8.38 (d, $^3J_{H,H}$ = 2.4 Hz, 2 H, α), 8.33 (d, $^3J_{H,H}$ = 8.1 Hz, 2 H, d), 8.15 (dd, $^3J_{H,H}$ = 5.6, 1.3 Hz, 2 H, f), 7.83 (ddd, $^3J_{H,H}$ = 8.7, 7.0, 1.0 Hz, 2 H, b), 7.65–7.60 (overlapping multiplets, 5 H, e, 3, α′), 7.48 (ddd, $^3J_{H,H}$ = 8.0, 7.0, 1.4 Hz, 2 H, c), 6.86 (dd, $^3J_{H,H}$ = 2.7, 2.4 Hz, 2 H, β), 6.82 (d, $^3J_{H,H}$ = 8.8 Hz, 2 H, a), 6.60 (dd, $^3J_{H,H}$ = 2.9, 2.3 Hz, 1 H, β′) ppm.

Syntheses of Dinuclear Complexes

[{Ru(tpm)(2,2′-bpy)}$_2$(μ-pz)](PF$_6$)$_4$ [13, (Rubpy)$_2$-pz]. Procedure (a) Compounds **5** (0.050 g, 0.064 mmol) and **8** (0.054 g, 0.064 mmol) were dissolved in CH_2Cl_2 and stirred at room temperature for 3 d. The solid that formed was filtered off, washed several times with diethyl ether, and vacuum dried (yield 0.075 g, 73%). **Procedure (b)** Compound **5** (0.050 g, 0.064 mmol) and pz (0.0026 g, 0.032 mmol) were dissolved in CH_2Cl_2 and stirred at room temperature for 3 d. The solid obtained was separated by filtration, washed several times with diethyl ether, and vacuum dried. (yield 0.041 g, 80%). $C_{44}H_{40}F_{24}N_{18}P_4Ru_2$ (1604.03): calcd. C 32.97, H 2.52, N 15.73; found C 33.38, H 2.82, N 15.65. IR: ν_{max} = 1606 (m), 1467 (m), 1448 (s), 1413 (s), 1288 (s), 1254 (m), 1059 (m), 761 (s), 731 (m), 608 (w) cm^{-1}. ^{1}H NMR (200 MHz, [D$_6$]acetone, 20 °C): δ = 9.82 (s, 2 H, δ), 8.89 (d, $^3J_{H,H}$ = 7.9 Hz, 4 H, d), 8.73 (d, $^3J_{H,H}$ = 3.0 Hz, 4 H, γ), 8.67 (d, $^3J_{H,H}$ = 5.7 Hz, 4 H, a), 8.56 (d, $^3J_{H,H}$ = 3.0 Hz, 2 H, γ′), 8.30 (ddd, $^3J_{H,H}$ = 8.0, 7.9, 1.4 Hz, 4 H, c), 8.17 (d, $^3J_{H,H}$ = 2.3 Hz, 4 H, α), 7.64 (ddd, $^3J_{H,H}$ = 8.0, 5.6, 1.1 Hz, 4 H, b), 7.58 (s, 4 H, 1), 6.92 (d, $^3J_{H,H}$ = 2.3 Hz, 2 H, α′), 6.83 (dd, $^3J_{H,H}$ = 2.9, 2.4 Hz, 4 H, β), 6.40 (dd, $^3J_{H,H}$ = 2.9, 2.4 Hz, 2 H, β′) ppm.

[{Ru(tpm)(2,2′-bpy)}$_2$(μ-4,4′-bpy)](PF$_6$)$_4$ [14, (Rubpy)$_2$-bpy]: Compound **14** was obtained, as a reddish brown solid, from either **5** (0.050 g, 0.064 mmol) and **9** (0.059 g, 0.063 mmol) (yield 0.081 g, 77%), or from **5** (0.050 g, 0.064 mmol) and 4,4′-bpy (0.0050 g, 0.032 mmol) (yield 0.045 g, 84%), by procedures (a) and (b) respectively, which are described above for complex **13**. $C_{50}H_{44}F_{24}N_{18}P_4Ru_2$ (1680.07): calcd. C 35.77, H 2.64, N 15.02; found C 35.98, H 2.86, N 14.75. IR: ν_{max} = 1617 (w), 1448 (m), 1412 (m), 1287 (m), 1259 (m), 761 (m), 669 (w), 608 (w) cm^{-1}. ^{1}H NMR (200 MHz, [D$_6$]acetone, 20 °C): δ = 9.89 (s, 2 H, δ), 9.01 (d, $^3J_{H,H}$ = 8.4 Hz, 4 H, d), 8.92 (d, $^3J_{H,H}$ = 5.7 Hz, 4 H, a), 8.81 (d, $^3J_{H,H}$ = 2.9 Hz, 4 H, γ), 8.61 (d, $^3J_{H,H}$ = 2.8 Hz, 2 H, γ′), 8.34 (ddd, $^3J_{H,H}$ = 8.4, 8.0, 1.4 Hz, 4 H, c), 8.32 (d, $^3J_{H,H}$ = 2.2 Hz, 4 H, α), 7.87 (d, $^3J_{H,H}$ = 6.9 Hz, 4 H, 1), 7.69 (ddd, $^3J_{H,H}$ = 8.1, 5.7, 1.3 Hz, 4 H, b), 7.58 (d, $^3J_{H,H}$ = 6.9 Hz, 4 H, 2)) 6.96 (d, $^3J_{H,H}$ = 2.2 Hz, 2 H, α′), 6.90 (dd, $^3J_{H,H}$ = 2.5, 2.4 Hz, 4 H, β), 6.45 (dd, $^3J_{H,H}$ = 2.7, 2.4 Hz, 2 H, β′) ppm.

[{Ru(tpm)(phen)}$_2$(μ-pz)](PF$_6$)$_4$ [15, (Ruphen)$_2$-pz]: Compound **15** was obtained, as a reddish brown solid, from either **6** (0.050 g, 0.062 mmol) and **10** (0.054 g, 0.062 mmol) (yield 0.077 g, 76%), or from **6** (0.050 g, 0.062 mmol) and pz (0.0026 g, 0.032 mmol) (yield 0.041 g, 80%), by procedures (a) and (b) respectively, which are described above for complex **13**. $C_{48}H_{40}F_{24}N_{18}P_4Ru_2$ (1652.03): calcd. C 34.92, H 2.44, N 15.27; found C 35.04, H 2.67, N 15.14. IR: ν_{max} = 3154 (m), 1609 (m), 1466 (m), 1442 (m), 1420 (s), 1301 (s), 1255 (m), 1069 (m), 836 (s), 761 (s), 558 (s) cm^{-1}. ^{1}H NMR (200 MHz, [D$_6$]acetone, 20 °C): δ = 9.91 (s, 2 H, δ), 9.02 (dd, $^3J_{H,H}$ = 5.4, 1.2 Hz, 4 H, a), 8.86 (dd, $^3J_{H,H}$ = 8.2, 1.2 Hz, 4 H, c), 8.77 (d, $^3J_{H,H}$ = 2.9 Hz, 4 H, γ), 8.52 (d, $^3J_{H,H}$ = 2.9 Hz, 2 H, γ′), 8.42 (s, 4 H, d), 8.29 (d, $^3J_{H,H}$ = 2.2 Hz, 4 H, α), 7.95 (dd, $^3J_{H,H}$ = 8.3, 5.3 Hz, 4 H, b), 7.21 (s, 4 H, 1), 6.85 (dd, $^3J_{H,H}$ = 2.8, 2.5 Hz, 4 H, β), 6.33 (d, $^3J_{H,H}$ = 2.3 Hz, 2 H, α′), 6.21 (dd, $^3J_{H,H}$ = 2.8, 2.4 Hz, 2 H, β′) ppm.

[{Ru(tpm)(phen)}$_2$(μ-4,4′-bpy)](PF$_6$)$_4$ [16, (Ruphen)$_2$-bpy]: Compound **16** was obtained, as a reddish brown solid, from either **6** (0.050 g, 0.062 mmol) and **11** (0.058 g, 0.062 mmol) (yield 0.081 g, 76%), or from **6** (0.050 g, 0.062 mmol) and 4,4′-bpy (0.0050 g, 0.032 mmol) (yield 0.045 mg, 84%), by procedures (a) and (b) respectively, which are described above for complex **13**. $C_{54}H_{44}F_{24}N_{18}P_4Ru_2$ (1728.07): calcd. C 37.55, H 2.57, N 14.60; found C 37.89, H 2.45, N 14.43. IR: ν_{max} = 1615 (m), 1450 (w), 1413 (s), 1286 (m), 1284 (w), 761 (m) cm^{-1}. ^{1}H NMR (200 MHz, [D$_6$]acetone, 20 °C): δ = 9.91 (s, 2 H, δ), 9.28 (dd, $^3J_{H,H}$ = 5.3, 1.3 Hz, 4 H, a), 8.93 (dd, $^3J_{H,H}$ = 8.2, 1.2 Hz, 4 H, c), 8.82 (d, $^3J_{H,H}$ = 3.0 Hz, 4 H, γ), 8.54 (d, $^3J_{H,H}$ = 3.0 Hz, 2 H, γ′), 8.52 (s, 4 H, d), 8.40 (d, $^3J_{H,H}$ = 2.3 Hz, 4 H, α), 8.03 (dd, $^3J_{H,H}$ = 8.2, 5.2 Hz, 4 H, b), 7.61 (dd, $^3J_{H,H}$ = 5.3, 1.5 Hz, 4 H, 1), 7.35 (dd, $^3J_{H,H}$ = 5.3, 1.5 Hz, 4 H, 2), 6.91 (dd, $^3J_{H,H}$ = 2.9, 2.4 Hz, 4 H, β), 6.35 (d, $^3J_{H,H}$ = 2.3 Hz, 2 H, α′), 6.24 (dd, $^3J_{H,H}$ = 2.9, 2.4 Hz, 2 H, β′) ppm.

[{Ru(tpm)(biq)}$_2$(μ-pz)](PF$_6$)$_4$ [17, (Rubiq)$_2$-pz]: Compound **17** was obtained, as a violet solid, from **7** (0.030 g, 0.034 mmol) and pz (0.0014 g, 0.017 mmol) (yield 0.024 mg, 78%) by procedure (b) described above for complex **13**. $C_{60}H_{48}F_{24}N_{18}P_4Ru_2$ (1804.10): calcd. C 39.97, H 2.68, N 13.98%; found C 40.13, H 2.81, N 13.74. IR: ν_{max} = 1508 (s), 1457 (s), 1411 (m), 1383 (m), 1290 (m), 1097 (m), 832 (w), 784 (w), 669 (m) cm^{-1}. ^{1}H NMR (200 MHz, [D$_6$]acetone, 20 °C): δ = 10.31 (s, 2 H, δ), 8.97 (d, $^3J_{H,H}$ = 3.0 Hz, 4 H, γ), 8.88 (s, 4 H, 1), 8.88 (d, 2 H, γ′), 8.34 (d, $^3J_{H,H}$ = 3.5 Hz, 4 H, f), 8.29 (dd, $^3J_{H,H}$ = 8.1, 1.4 Hz, 4 H, d), 8.18 (d, $^3J_{H,H}$ = 2.4 Hz, 4 H, α), 8.09 (d, $^3J_{H,H}$ = 3.5 Hz, 4 H, e), 7.78 (m, 4 H, b), 7.63 (d, $^3J_{H,H}$ = 2.3 Hz, 2 H, α′), 7.41 (m, 4 H, c), 6.84 (m, 4 H, β), 6.74 (d, $^3J_{H,H}$ = 8.9 Hz, 4 H, a), 6.58 (m, 2 H, β′) ppm.

[{Ru(tpm)(biq)}$_2$(μ-4,4′-bpy)](PF$_6$)$_4$ [18, (Rubiq)$_2$-bpy]: Compound **18** was obtained, as a violet solid, from either **7** (0.030 g, 0.034 mmol) and **12** (0.035 g, 0.034 mmol) (yield 0.045 g, 70%), or from **7** (0.053 g, 0.060 mmol) and 4,4′-bpy (0.0047 g, 0.030 mmol) (yield 0.047 g, 83%), by procedures (a) and (b) respectively, which are described above for complex **13**. $C_{66}H_{52}F_{24}N_{18}P_4Ru_2$ (1880.13): calcd. C 42.18, H 2.79, N 13.42; found C 41.98, H 2.64, N 13.05. IR: ν_{max} = 1509 (w), 1411 (m), 1287 (m), 1257 (w), 1099 (m), 1056 (w), 1020 (w), 787 (m) cm^{-1}. ^{1}H NMR (200 MHz, [D$_6$]acetone, 20 °C): δ = 10.65 (s, 2 H, δ), 8.97 (d, $^3J_{H,H}$ = 2.6 Hz, 4 H, γ), 8.90 (d, $^3J_{H,H}$ = 2.5 Hz, 2 H, γ′), 8.76 (d, $^3J_{H,H}$ = 8.6 Hz, 4 H, 1), 8.64 (d, $^3J_{H,H}$ = 8.7 Hz, 4 H, 2), 8.26 (dd, $^3J_{H,H}$ = 8.3, 1.0 Hz, 4 H, d), 8.22 (d, $^3J_{H,H}$ = 2.3 Hz, 4 H, α), 8.03 (dd, $^3J_{H,H}$ = 5.8 Hz, 4 H, f), 7.77 (m, 4 H, b), 7.58 (d, $^3J_{H,H}$ = 2.1 Hz, 2 H, α′), 7.44–7.40 (overlapping multiplets, 8 H, c, e), 6.77 (m, 4 H, β), 6.74 (d, $^3J_{H,H}$ = 8.4 Hz, 4 H, a), 6.55 (m, 2 H, β′) ppm.

Electrochemistry and Spectroelectrochemistry: Electrochemical experiments were carried out with argon-purged acetonitrile solutions of the samples with an Autolab PGSTAT 12 potentiostat/galvanostat instrument interfaced to a personal computer, with cyclic voltammetry (CV) and differential pulse voltammetry (DPV) techniques. The working electrode was a glassy carbon electrode (0.08 cm^2, Amel); its surface was polished immediately prior to use with a 0.05 µm alumina-water slurry on a felt surface. The counter electrode was a Pt wire. We used an Ag wire as a quasi-reference electrode, and we added 5 mL of a 0.1 M solution of ferrocene in acetonitrile to act as an internal standard. The concentration of the examined compounds was 5.0×10^{-4} M; tetraethylammonium hexafluorophosphate 0.05 M was added as a supporting electrolyte. Cyclic voltammograms were obtained at sweep rates of 20, 50, 200, and 500 mV s^{-1}; DPV experiments were performed with a scan rate of 4 mV s^{-1}, a pulse height of 10 mV, and a duration of 40 ms. The ferrocene/ferrocenium measured potential vs. SCE, under the experimental conditions employed, was 0.395 V. For reversible processes the half-wave potential values are reported; the same values are obtained from the DPV peaks and from an average of the cathodic and anodic cyclic voltammetric peaks. For irreversible processes the reported values are those evaluated from the peak potentials recorded in the DPV experiments. Both CV and DPV techniques have been used to measure the number of the exchanged electrons involved in each redox process. No reliable conclusions can be drawn on the number of electrons exchanged in irreversible processes. To establish the reversibility of a process, the following criteria were considered: (i) separation between cathodic and anodic peaks, (ii) close to unity ratio of the intensities of the cathodic and anodic currents, and (iii) constancy of the peak potential on changing the sweep rate in the cyclic voltammograms. For the redox potentials the estimated errors are ± 10 mV.

Spectroelectrochemical measurements were recorded on a JASCO V570 spectrophotometer connected to an EG&G 273A potentiostat.

Absorption and Luminescence Spectra: Absorption spectra were recorded with a JASCO V570 spectrophotometer. Luminescence spectra were recorded on a Jobin Yvon-Spex Fluoromax 2 spectrofluorimeter equipped with a Hamamatsu R3896 photomultiplier, and the spectra were corrected for photomultiplier response with a program purchased with the fluorimeter. Luminescence lifetimes were determined by time-correlated single-photon-counting (TCSPC) with an Edinburgh OB900 spectrometer (a 408 nm light pulse was generated with a Hamamatsu PL2 laser diode, with a pulse width of 59 ps). Experimental uncertainties are as follows: absorption maxima, 2 nm; molar absorption coefficient, 10%; emission maxima, 5 nm; excited state lifetimes, 10%).

Supporting Information (see footnote on the first page of this article): Syntheses and characterization of complex metals **2**–**7**, interpreted ^{1}H NMR spectra of complexes **8**, **9**, **11**–**14**, and **16**–**18**.

Acknowledgments

G. D. is indebted to helpful colleagues, and particularly to Professor C. A. Veracini, Head of the Chemistry and Industrial Chemistry Department of the University of Pisa, for the free use of NMR instruments. M. G. is grateful to the University of Pisa for the award of a doctoral scholarship.

---

[1] For recent reviews, see: a) J. G. Vos, J. M. Kelly, *Dalton Trans.* **2006**, 4869–4883; b) S. Campagna, F. Puntoriero, F. Nastasi, G. Bergamini, V. Balzani, *Top. Curr. Chem.* **2007**, *280*, 117–214; c) V. Balzani, A. Credi, M. Venturi, *ChemSA* **2008**, *1*, 26–58.

[2] a) S. Serroni, G. Denti, *Inorg. Chem.* **1992**, *31*, 4251–4255, and references cited therein. b) G. Denti, S. Campagna, S. Serroni, M. Ciano, V. Balzani, *J. Am. Chem. Soc.* **1992**, *114*, 2944–2950; c) V. Balzani, S. Campagna, G. Denti, A. Juris, S. Serroni, M. Venturi, *Coord. Chem. Rev.* **1994**, *132*, 1–13, and references cited therein d) V. Balzani, S. Campagna, G. Denti, A. Juris, S. Serroni, M. Venturi, *Acc. Chem. Res.* **1998**, *31*, 26–34, and references cited therein e) M. Sommovigo, G. Denti, S. Serroni, S. Campagna, C. Mingazzini, C. Mariotti, A. Juris, *Inorg. Chem.* **2001**, *40*, 3318–3323.

[3] a) E. Baranoff, J. P. Collin, L. Flamigni, J.-P. Sauvage, *Chem. Soc. Rev.* **2004**, *33*, 147–155; b) H. Hofmeier, U. S. Schubert, *Chem. Soc. Rev.* **2004**, *33*, 373–399; c) U. S. Schubert, H. Hofmeier, G. R. Newkome, in: *Modern Terpyridine Chemistry*, Wiley-VCH, Weinheim, Germany, **2006**; d) R. A. Fallahpour, *2,2′:6′,2′′-Terpyridines, its metallodendrimers*, www.hetcat.com, **2003**; e) M. I. J. Polson, E. A. Medlycott, G. S. Hanan, L. Mikelsons, N. J. Taylor, M. Watanabe, Y. Tanaka, F. Loiseau, R. Passalacqua, S. Campagna, *Chem. Eur. J.* **2004**, *10*, 3640–3648; f) M. W. Cooke, G. S. Hanan, F. Loiseau, S. Campagna, M. Watanabe, Y. Tanaka, *J. Am. Chem. Soc.* **2007**, *129*, 10481–10488, and references cited therein; g) F. Nastasi, F. Loiseau, S. Campagna, E. A. Medlycott, M.-P. Santoni, G. S. Hanan, *Can. J. Chem.* **2009**, *87*, 254–263, and references cited therein.

[4] a) M. Onishi, K. Ikemoto, K. Hiraki, *Inorg. Chim. Acta* **1991**, *190*, 157–159; b) M. Onishi, M. Yamaguchi, S. Kumagae, H. Kawano, Y. Arikawa, *Inorg. Chim. Acta* **2006**, *359*, 990–997.

[5] F. R. Keene, M. R. Snow, P. J. Stephenson, E. R. T. Tiekink, *Inorg. Chem.* **1988**, *27*, 2040–2045.

[6] For a general review on tpm complexes of transition metals, see: H. R. Bigmore, S. C. Lawrence, P. Mountford, C. S. Tredget, *Dalton Trans.* **2005**, 635–651.

[7] K. R. Barqawi, A. Llobet, T. J. Meyer, *J. Am. Chem. Soc.* **1988**, *110*, 7751–7759.

[8] a) F. Laurent, E. Plantalech, B. Donnadieu, A. Jiménez, F. Hernándezc, M. Martínez-Ripoll, M. Biner, A. Llobet, *Polyhedron* **1999**, *18*, 3321–3331; b) J. M. Calvert, R. H. Schmehl, B. P. Sullivan, J. S. Facci, T. Meyer, R. W. Murray, *Inorg. Chem.* **1983**, *22*, 2051–2062.

[9] a) C. Metcalfe, H. Adams, I. Haq, J. A. Thomas, *Chem. Commun.* **2003**, 1152–1153; b) P. Waywell, V. Gonzalez, M. R. Gill, H. Adams, A. J. H. M. Meijer, M. P. Williamson, J. A. Thomas, *Chem. Eur. J.* **2010**, *16*, 2407–2417; c) S. P. Foxon, C. Metcalfe, H. Adams, M. Webb, J. A. Thomas, *Inorg. Chem.* **2007**, *46*, 409–416.

[10] N. E. Katz, I. Romero, A. Llobet, T. Parella, J. Benet-Bucholz, *Eur. J. Inorg. Chem.* **2005**, 272–277.

[11] a) F. Falgade, M. E. García Posse, M. M. Vergara, M. Cattaneo, N. E. Katz, I. Romero, T. Parrella, A. Llobet, *Polyhedron* **2007**, *26*, 17–23; b) G. Pourrieux, F. Fagalde, N. E. Katz, T. Parella, J. Benet-Buchholz, A. Llobet, *Polyhedron* **2008**, *27*, 2990–2996.

[12] C. Metcalfe, I. Haq, J. A. Thomas, *Inorg. Chem.* **2004**, *43*, 317–323.

[13] A. Llobet, P. Doppelt, T. J. Meyer, *Inorg. Chem.* **1988**, *27*, 514–520.

[14] H. Taube, *Pure Appl. Chem.* **1979**, *51*, 901–912.

[15] a) P. K. Byers, F. G. A. Stone, *J. Chem. Soc., Dalton Trans.* **1991**, 93–100; b) A. R. Katritzky, A. E. Abdel-Rahman, D. E. Leahy, O. A. Schwarz, *Tetrahedron* **1983**, *39*, 4133–4142; c) P. K. Byers, A. J. Canty, R. T. Honeyman, R. M. Claremont, C. Lopez, J. L. Lavandera, J. Elguero, *Gazz. Chim. Ital.* **1992**, *122*, 341; d) J. Guerrero, L. Farías, L. L. Lemus, A. Quintanilla, A. Mena, L. Cortez, R. F. Baggio, M. T. Garland, *Polyhedron* **2006**, *25*, 9–16.

[16] J.-C. Chambron, J.-P. Sauvage, E. Amouyal, P. Koffi, *Nouv. J. Chim.* **1985**, *9*, 527–529.

[17] V. Balzani, A. Juris, F. Barigelletti, P. Belser, A. von Zelewsky, *Riken Q.* **1984**, *78*, 78–85.

[18] A. Kirsch-De Mesmaeker, R. Nasielski-Hinkens, D. Maetens, D. Pauwels, J. Nasielski, *Inorg. Chem.* **1984**, *23*, 377–379.
[19] a) G. Denti, S. Campagna, L. Sabatino, S. Serroni, M. Ciano, V. Balzani, *Inorg. Chem.* **1990**, *29*, 4750–4758; b) V. Balzani, A. Juris, M. Venturi, S. Campagna, S. Serroni, *Chem. Rev.* **1996**, *96*, 759–833, and references cited therein.
[20] C. Creutz, H. Taube, *J. Am. Chem. Soc.* **1969**, *91*, 3988–3989.
[21] N. Dowling, P. M. Henry, N. A. Lewis, H. Taube, *Inorg. Chem.* **1981**, *20*, 2345–2348.
[22] V. Balzani, P. Ceroni, A. Juris, M. Venturi, S. Campagna, F. Puntoriero, S. Serroni, *Coord. Chem. Rev.* **2001**, *219–221*, 545–572, and references cited therein.
[23] M. Klessinger, J. Michl, in: *Excited States, Photochemistry of Organic Molecules*, Wiley-VCH, New York, **1995**.
[24] a) R. Englman, J. Jortner, *J. Mol. Phys.* **1970**, *18*, 145–164; b) B. R. Henry, W. Siebrand, in: *Organic Molecular Photophysics* (Ed.: J. B. Birks), vol. 1, Wiley, New York, **1973**; c) J. V. Caspar, E. M. Kober, B. P. Sullivan, T. J. Meyer, *J. Am. Chem. Soc.* **1982**, *104*, 630–632; d) P. Chen, T. J. Meyer, *Chem. Rev.* **1998**, *98*, 1439–1477; e) J. V. Caspar, T. J. Meyer, *J. Am. Chem. Soc.* **1983**, *105*, 5583–5590; f) J. P. Claude, T. J. Meyer, *J. Phys. Chem.* **1995**, *99*, 51–54; g) N. H. Damrauer, T. R. Boussie, M. Devenney, J. K. McCusker, *J. Am. Chem. Soc.* **1997**, *119*, 8253–8268; h) J. A. Treadway, G. F. Strouse, R. R. Ruminski, T. J. Meyer, *Inorg. Chem.* **2001**, *40*, 4508–4509; i) Y.-Q. Fang, N. J. Taylor, F. Laverdière, G. S. Hanan, F. Loiseau, F. Nastasi, S. Campagna, H. Nierengarten, E. Leize-Wagner, A. Van Dorsselaer, *Inorg. Chem.* **2007**, *46*, 2854–2863.
[25] F. Loiseau, S. Serroni, S. Campagna, *Collect. Czech. Chem. Commun.* **2003**, *68*, 1677–1686.
[26] C. Creutz, *Prog. Inorg. Chem.* **1983**, *30*, 1–74.
[27] C. Lambert, G. Nöll, *J. Am. Chem. Soc.* **1999**, *121*, 8434–8442, and references cited therein.
[28] N. S. Hush, *Prog. Inorg. Chem.* **1967**, *8*, 391–444.
[29] *Chem. 3D*, CambridgeSoft, Cambridge, USA (software based on the MM2 Force Field method).
[30] C. A. Bignozzi, R. Argazzi, J. R. Schoonover, K. C. Gordon, R. B. Dyer, F. Scandola, *Inorg. Chem.* **1992**, *31*, 5260–5267.
[31] a) D. E. Richardson, H. Taube, *J. Am. Chem. Soc.* **1983**, *105*, 40–51; b) R. C. Rocha, H. E. Toma, *Polyhedron* **2003**, *22*, 1303–1313.
[32] D. L. Reger, T. C. Grattan, K. J. Brown, C. A. Little, J. J. S. Lamba, A. L. Rheingold, R. D. Sommer, *J. Organomet. Chem.* **2000**, *607*, 120–128.

Received: September 9, 2010